Proceedings of the 13th International Conference on Pattern Recognition - ICPR'96,
IEEE Computer Society Press, Los Alamitos, California, vol. 2, pp. 285-289.

Classification of Irregularly Shaped Micro-Objects Using Complex Fourier Descriptors

Volodymyr V. Kindratenko and Pierre J. M. Van Espen
Micro- and Trace Analysis Center (MiTAC), University of Antwerp (UIA)
Universiteitsplein 1, B-2610 Wilrijk, Belgium

Abstract

A new method for characterizing complex irregular shapes of natural objects (e.g. plant cells, aerosol particles) is presented. The method employs complex Fourier analysis rather than the traditional forms of the Fourier analysis. Digitized images of objects are processed and the contours are tracked by a classical boundary following technique. A new contour pre-processing technique allows to normalize position, size and orientation of a contour. A new contour resampling technique results in a more precise polygonal approximation of the contour. The resampled contour is represented in a complex plane and its complex Fourier coefficients are computed. The technique is applied to the classification of individual algae cells and their agglomerates employing two different classification methods: hierarchical clustering and neural network. The results demonstrate the applicability of the method for the classification of complex irregular shapes.

1. Introduction

The fundamental problem of shape quantification and classification is related to the difficulty of finding variables that unambiguously describe and discriminate the shape characteristics of objects regardless their size and orientation. Currently a large number of shape analysis methods are being used. The most commonly applied are based on Fourier coefficients, chain coding, fractal dimensions and dynamic shape factors. A general method has not been developed so far.

The variety of the methods for shape characterization is explained by the large number of particular problems in this field. Each method mainly relates to its own class of problems. E.g. fractal analysis, being an appropriate tool for characterization of complicated shapes, cannot be applied in a case of regular shapes. Moreover, the use of fractal analysis often requires human interaction. The dynamic shape factors, introduced by Medalia [1], serve as another example. This method is based on the representation of a shape as an ellipsoid with equivalent radii of gyration about the central principal axes. In some cases this method is not sensitive enough; different shapes may result in similar shape factors. Both methods attempt to condense all the details of the shape into a single number. However, there can be an infinite number of visually different shapes having the same fractal dimension or similar shape factors. Alternatively it is possible to represent the shape with a set of numbers so that enough information is preserved to reconstruct the shape with sufficient precision. Fourier analysis is a common approach of such representation. Its classical (R, θ) form is useful in case of non re-entrant shapes but is almost useless in the case of re-entrant shapes [2]. The chain coding is a shape unrolling technique producing a list of numbers which can be interpreted as the changes of slope vs. position along the particle's silhouette edge. Chain code representation of the shape in combination with Fourier analysis is very effective method which allows to avoid problem with re-entrant shapes. It is proved to be successful in a surprising number of cases [3].

The above mentioned Fourier analyses methods require reduction of the number of Fourier coefficients. Normally only the first 10 to 20 coefficients are used for analysis and classification [2]. Contours reconstructed with the first 10 - 20 coefficients are well-smoothed versions of the original ones. Of course, such reduction leads to the loss of information contained in the contour. On the other hand it is possible to reduce the total number of points of the contour and keeping all Fourier coefficients. One way of doing this is to resample the contour at a finite number of points, put them into the complex plain and calculate the corresponding complex Fourier descriptor (CFD). Such descriptors were successfully used by many researchers for characterization and classification of various objects having pre-defined shapes (e.g. aircraft [4]). Normally an iterative type of classification algorithms is employed [4], which searches for the optimum match between the unknown shape and each reference shape. For a number of classification problems such as the classification of natural objects

(aerosol particles, plant cells, etc.) those algorithms are ineffective. Either such a library does not exists, or one wants to perform an unsupervised classification without using a library of reference shapes. Up to our knowledge only one attempt has been made to adopt CFDs for the classification of natural objects (quarts grains) [5]. In this application a large number of Fourier coefficients (256) were computed and additional statistical tests were applied to reduce the number of coefficients prior to classification. In this article we propose and test another approach to obtain and use the CFDs for the classification of the irregular complex shapes. The method employs a simple procedure to normalize the position, size and orientation of the contour, rather than the complicated complex Fourier coefficients preprocessing. Also a more precise contour resampling technique is employed instead of the simple, but inaccurate, resampling techniques normally used. In this way the number of complex Fourier coefficients used for classification is effectively reduced. For the classification of the shapes, unsupervised classification algorithms are adopted rather than iterative ones used for the pre-defined shape recognition.

2. Method

2.1. Complex Fourier descriptors

From a digitized image of an object the contour is obtained using the classical method described in [6]. This contour consists of the L points $(x(j), y(j))$ in Euclidean space. We can consider this closed contour C in the complex plane. A point moving along the contour generates a discrete periodic complex function

$$c(j) = x(j) + iy(j) \qquad (1)$$

with $j = 0, 1, \ldots, L-1$.

The discrete complex Fourier series expansion of $c(j)$ is given by

$$c(j) = \sum_{k=0}^{L-1} A_k e^{2\pi \frac{ikj}{L}} \qquad (2)$$

where the coefficients A_k are obtained as the discrete complex Fourier transform

$$A_k = \frac{1}{L} \sum_{j=0}^{L-1} c(j) e^{2\pi \frac{-ikj}{L}} \qquad (3)$$

The sequence of complex coefficients $\{A_k\}$ is the *complex Fourier descriptor* (CFD) of the given contour.

In order to apply CFDs for shape classification some additional processing is required.

2.2. Contour preprocessing

The shape descriptors should be invariant to rotation, size and position differences in order to use them for classification purposes. This can be done by normalizing the CFDs after that they have been obtained [4, 5]. However, this normalization procedure of the CFDs is difficult especially for rotation and shift of the origin. Therefor we normalize the contour instead of normalization of its CFD.

The contour's center of mass (x_m, y_m) is determined and new contour coordinates are calculated as follows:

$$(x_{new}(j), y_{new}(j)) = (x(j) - x_m, y(j) - y_m) \qquad (4)$$

After this translation the contour's center of mass will have the coordinates (0, 0).

To normalize the size of the contour, the largest distance d from the center of mass to the contour is calculated and the new, normalized contour coordinates are calculated as follows:

$$(x_{new}(j), y_{new}(j)) = \left(\frac{x(j)}{d}, \frac{y(j)}{d} \right) \qquad (5)$$

Normalization of the orientation and location of the starting-point of a contour is done as follows. The point (x', y') of a contour for which the distance d to the center of mass is largest is found and the contour is rotated around the center of mass as follows:

$$x_{new}(j) = \sqrt{x(j)^2 + y(j)^2} \cos(\alpha + \beta(j)) \qquad (6)$$

$$y_{new}(j) = \sqrt{x(j)^2 + y(j)^2} \sin(\alpha + \beta(j)) \qquad (7)$$

where $\beta(j)$ is the angle between the vectors $\overrightarrow{(x(j), y(j))}$ and $\overrightarrow{(1,0)}$ and α is the angle between the vectors $\overrightarrow{(x', y')}$ and $\overrightarrow{(1,0)}$. After this rotation the point (x', y') is moved to the position (1, 0) and will be used as the starting point of the contour.

2.3. Contour resampling

The number of the complex Fourier coefficients needed to reconstruct the contour equals to the number of the points of the contour L. In practice such description is too large for classification purposes. Moreover CFDs of different contours may have a different number of the coefficients so they cannot be compared. To eliminate these problems the contour should be resampled to make the total number of the contour's points, L^*, equal for all contours and as small as possible.

Thomas et. al [5] proposed to do the resampling simply by taking every L/L^* point of the contour. Our resampling technique is essentially different in the way the L^* points of the resampled contour are obtained. First, the

curvature at every point of the contour is computed using the median filtered differencing as described in [7]. Second, the point of the contour at which the amplitude of the curvature is largest is determined and added to the list of the points forming the new, resampled contour. Third, the L/L^* nearest neighborhood points (in the original the contour) of the found point are excluded from the further analysis. Steps 2 and 3 are repeated until L^* points of the reconstructed contour are found. The graph in Fig. 1b shows the curvature of the contour depicted in Fig. 1a. The L^* points (found as described above) are labeled with '**o**' (L = 1437, L^* = 64). Only those points were used for the reconstruction of the resampled contour shown in Fig. 1c.

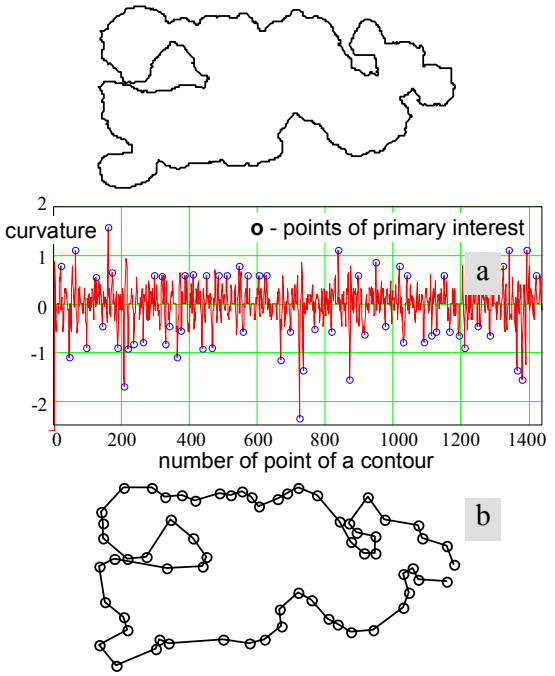

Fig. 1. (a) contour of an algae cell agglomerate contains 1437 points; (b) plot of the curvature of the contour depicted in a; the points with highest curvature in certain intervals are labeled with 'o'; the corresponding contour points make up the resampled contour; (c) resampled contour with 64 points.

This resampling technique minimizes the loss of information and allows to reduce the total number of contour points to a reasonably small number. The resampled contour is a polygon approximation of the real shape. Such an approximation is more robust and preserves more details compared to resampling at equally spaced intervals which results in a smoothed representation.

2.4. Classification algorithms

After performing the normalization and resampling, the CFD of the contour can be computed using Eq. 3 and applied directly for classification. However, in practice it is more convenient to use the sequence of modules of A_k, $\{|A_k|\}$, as shape descriptor, avoiding the need to handle complex numbers.

Supervised and unsupervised methods were used to test the applicability of the shape descriptor $\{|A_k|\}$, derived as discussed above, for shape classification. Unsupervised classification was performed using hierarchical cluster analysis [8] as implemented in the IDAS software [9]. Supervised classification was performed with a three-layer feedforward neural network which was trained using the stochastic back propagation training technique [10]. This part of the work was done using the NeuFrame software [11].

3. Application

Fig. 2 shows scanning electron microscopy images of an individual algae cell and a cell agglomerate. During further automated analysis one is only interested in individual cells, creating the need to differentiate automatically between individual cells and cell agglomerates.

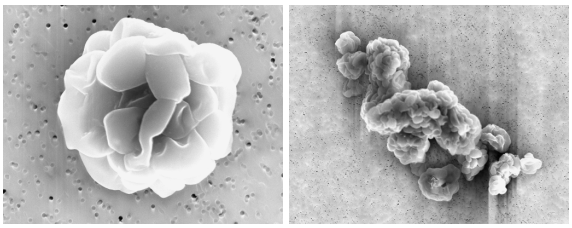

Fig. 2. Scanning electron micrographs on an individual algae cell (a) and a cell agglomerate (b)

A small collection of 30 scanning electron microscopy images: 24 images of individual sells and 6 images of cell agglomerates was used. Binary images were obtained by a technique described in [12] and the contour following technique [6] was employed to extract the contours of the objects under study. The shape descriptor $\{|A_k|\}$ with 64 coefficients was obtained for each object, using the contour preprocessing and resampling methods which were described above. Fig. 1c shows an example of the normalized and resampled contour of an algae agglomerate. The $\{|A_k|\}$ obtained for an agglomerate and an individual cell are shown in Figs 3a and 3b respectively.

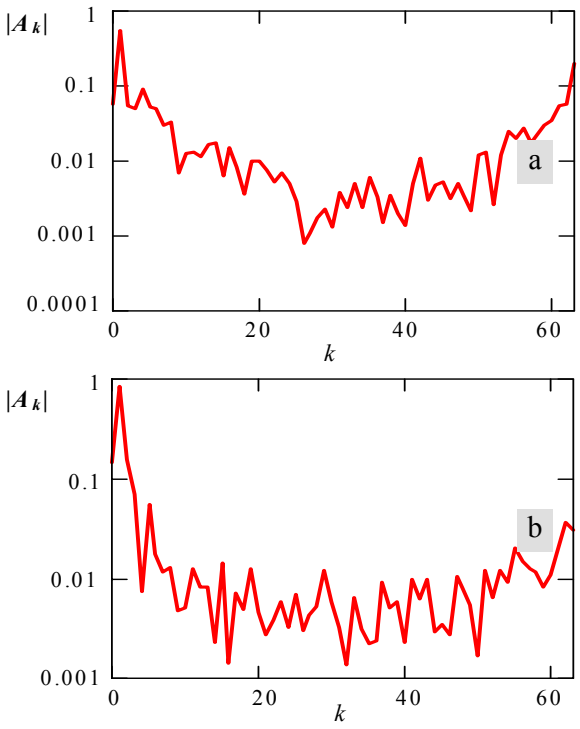

Fig. 3. The calculated shape descriptors $\{|A_k|\}$ for an agglomerate of algae cells (a) and for an individual algae cell (b).

A quantitative analysis of the population of the individual cells and agglomerates was performed using hierarchical clustering. The dendrogram, representing the results of hierarchical clustering is shown in Fig. 4.

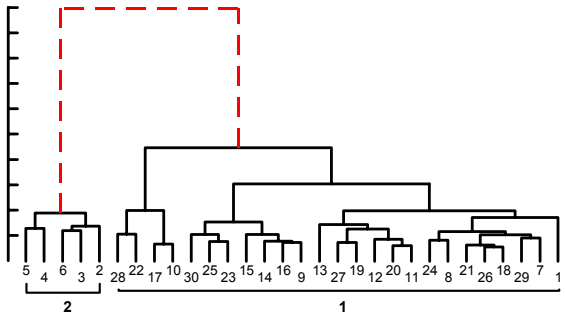

Fig. 4. Dendrogram showing the results of the hierarchical clustering of algae cells and cell agglomerates. Cell agglomerates are labeled from 1 to 6, individual cells are labeled from 7 to 30. Agglomerate #1 is misclassified.

The presence of the two classes of objects is evident from this dendrogram. One agglomerate was classified as belonging to the class of individual cells due to the nearly rounded shape of this agglomerate.

In practice it is more relevant to classify individual objects rather than to perform a quantitative analysis of a population. This was done using a three-layer feedforward network. A schematic representation and some characteristics of the network are given in Fig. 5. For the input layer a linear transfer function was used, whereas for the hidden layer and the output layer sigmoidal transfer functions were used.

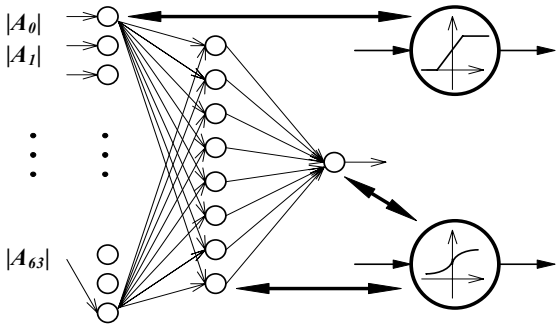

Fig. 5. Schematic representation of the neural network used.

The network was trained using the back-propagation training technique on a very limited training set consisting of the shape descriptors $\{|A_k|\}$ of 3 randomly chosen cell agglomerates and 6 randomly chosen individual cells. At the output layer 0 corresponded to agglomerates and 1 to individual cells. A random error of 0.01 was added to the training set during the training of the neural network. The training was performed until the error reached its lowest value of 0.05 after 612 complete passes through the set of training data. The error graph of the training cycle is given in Fig. 6.

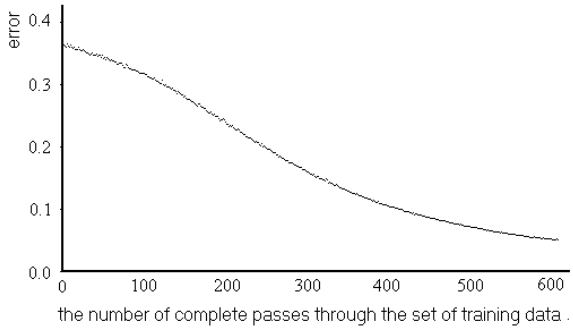

Fig. 6. Error graph obtained during the training of the network.

Next the set of 30 shape descriptors $\{|A_k|\}$ was given to the trained network. The results of the corresponding outputs of the network are represented graphically in Fig. 7. For all algae cell agglomerates the network output is lower than 0.6 whereas for all individual cells the output is larger than 0.7.

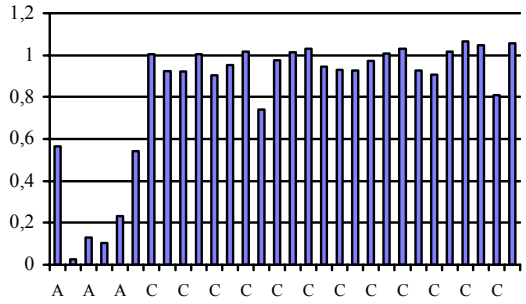

Fig. 7. Outputs of the trained network for the cells (C) and cell agglomerates (A).

4. Conclusion

The concept of complex Fourier coefficients was used by many researches for the classification and recognition of *pre-defined* shapes. This work describes a new approach for obtaining complex Fourier descriptors that are invariant to position, size and orientation and are based on a more optimum resampling strategy. The complex Fourier coefficients can be used for classification and recognition of *complex irregular* shapes (plant cells, aerosol particles, etc.). Examples of supervised and unsupervised classifications of algae cells and their agglomerates show the practical applicability of the method.

References

1. A.I. Medalia, Dynamic Shape Factors of Particles, Powder Technology, 1970/71, vol. 4, pp. 117 - 138.
2. R. Ehrlich, B. Weinberg, An Exact Method for Characterization of Grain Shape, Journal of Sedimentary Petrology, 1970, vol. 40, pp. 205 - 212.
3. J.C. Russ, The Image Processing Handbook, 2nd edition, CRC Press, Boca Raton, Florida, 1995.
4. T.P. Wallace, P.A. Wintz, An Efficient Three-Dimensional Aircraft Recognition Algorithm Using Normalized Fourier Descriptors, Computer Graphics and Image Processing, 1980, vol. 13, pp. 99 - 126.
5. M.C. Thomas, R.J. Wiltshire, A.T. Williams, The Use of Fourier Descriptors in the Classification of Particle Shape, Sedimentology, 1995, vol. 42, pp. 635 - 645.
6. A. Rosenfeld, A.C Kak, Digital Picture Processing vol. 2, Academic Press, London, 1982.
7. J. Matas, Z. Shao, J. Kittler, Estimation of Curvature and Tangent Direction by Median Filtered Differencing, Lecture Notes in Computer Science (Proceedings of 8th International Conference on Image Analysis and Processing - ICIAP'95), 1995, vol. 974, pp. 83-88.
8. M. Mellou, J. Militky, M. Forina, Chemometrics for Analytical Chemistry vol. 1, 2nd edition, Ellis Horwood Limited, New York, 1992.
9. I. Bondarenko, B. Treiger, P. Van Espen, R. Van Grieken, IDAS, a Windows-Based Software Package for Cluster Analysis, Spectrochimica Acta B51, 1996, pp. 441 - 456.
10. J.M. Zurada, Introduction to Artificial Neural Systems, West Publishing Company, New York, 1992.
11. NCS Company, Totton, UK; World Wide Web: http://www.demon.co.uk/skylake.
12. A.D. Brink, Gray-level Thresholding of Images Using a Correlation Criterion, Pattern Recognition Letters, 1989, vol. 9, pp. 335 - 341.